Loran of the Future – On-Air Tests of Some Possible Changes

Prof. Peter F. Swaszek, University of Rhode Island

Capt. Richard Hartnett, PhD, U.S. Coast Guard Academy

Dr. Gregory W. Johnson, Ruslan Shalaev, and Christian Oates, Alion Science & Technology

ABSTRACT

The specifications of the Loran-C system have remained static over the past 50 years: a teardrop shaped pulse, 8 pulses in a group (9 for Master), a set of Group Repetition Intervals, a two group Phase Code Interval with fixed Master and Secondary phase codes, etc. Over this history there have been examinations of how changes to the system might improve or extend performance, but these basics are unchanged. As part of the move to *e*Loran, it is time to evaluate the impact of potential changes and embed those of value into the new system.

During the summer and fall of 2008, these authors have tested a new transmitter for *e*Loran, installed temporarily at the Loran Support Unit, in order to determine whether it meets both the existing Loran signal specification and the envisioned *e*Loran specification. Part of this testing time also allowed for on-air implementation of potential changes to the *e*Loran signal. This paper, as a follow-up of prior work by these authors, investigates and tests possible changes to the 9th pulse Loran Data Channel's modulation set and Loran's phase codes and examines what improvements the changes could provide.

INTRODUCTION

The specifications of the Loran-C system have remained static over the past 50 years: a teardrop shaped pulse, 8 pulses in a group (9 for Master), a set of Group Repetition Intervals (GRIs), a two group Phase Code Interval (PCI) with fixed Master and Secondary phase codes, etc. Over this history there have been examinations of how changes to the system might improve or extend performance, but these basics are unchanged. As part of the move to *e*Loran, it is time to evaluate the impact of potential changes and embed those of value into the new system. The two changes of interest in this paper are adding data carrying capacity and new phase codes:

- Significant research effort has been spent in recent years on adding data communications capacity to the Loran signals – the so called Loran Data Channel (LDC). This effort included Clarinet Pilgrim in the 1960s, Eurofix which has been transmitting on stations in Europe since 1997, IFM which was tested in the US in the early 2000s, and 9th pulse LDC which is currently operating on 8 stations within CONUS. Of late, there have been discussions on how to increase the data rate of the LDC.
- There has also been discussion on how the Loran phase code/GRI combination impacts cross rate interference (CRI). While work on new phase code and GRI combinations started in the 1970s, and the present authors revisited this issue earlier this year with a paper at PLANS 2008, there is no current plan to alter the phase codes.

During the summer and fall of 2008, these authors have tested a new transmitter for *e*Loran, installed temporarily at the Loran Support Unit, in order to determine whether the transmitter meets both the existing Loran signal specification and the envisioned *e*Loran specification. Part of this testing time also allowed for on-air implementation of potential changes to both the 9th pulse LDC and phase codes to test their efficacy. The tests considered the following:

LDC: Current 9th pulse LDC adds a single pulse to each Loran group; using pulse position modulation, each group transmits 5 bits of raw data. After Reed-Solomon coding to mitigate channel errors, the resulting data throughput is between 18.7 and 31.6 bits/sec, depending upon the GRI. It has been questioned in several venues if that rate is high enough for envisioned applications. Possible solutions that have been suggested include adding a 10th pulse and/or transmitting LDC on both rates of dual rated stations (combined, these could potentially quadruple the data rate). Another option is to increase the data rate per pulse by increasing the number of pulse positions. Both options are discussed below.

Phase codes: It was noted in the 1970s, and reemphasized by the current authors earlier this year, that the current Master and Secondary phase codes allow spectral overlap in transmissions from different Loran chains (minimally, there are common spectral lines at frequencies of 90, 95, 100, 105, and 110 kHz for all existing US rates; some pairs of chains share additional spectral lines). The result is that it is effectively impossible to remove all energy from an interfering chain through averaging; receivers must implement additional non-linear processing to produce unbiased data for the position solution algorithm. Further, it has been noted that simple changes to the phase codes, notably balancing on the two groups, would cancel most or all of these overlaps. A detailed analysis of this bias is presented below; testing with the new transmitter allowed demonstration of these effects.

This paper starts with an extremely brief review of Loran itself, followed by separate discussions of adding bits to 9th pulse LDC and the impact of the current unbalanced phase codes. Both of these sections begin with definitions relevant to the problem, include a review of prior work, and present new analyses and testing results.

LORAN 099 – THE BRIEFEST INTRODUCTION

As a navigation system, Loran is based upon the transmission of the "Loran pulse" as shown in Figure 1; a tear-drop shaped envelope (the envelope is proportional to $t^2 e^{-2t/65}$, shown in blue in the figure and normalized for unit maximum) modulated by a 100 kHz sinusoid. The important axis in the figure is the abscissa, showing time in μsec (the ordinate is less important since received signal strength will vary with power of the transmitter and distance from it).

A Loran transmitter broadcasts a "group" of 8 such pulses spaced 1000 μsec apart (if the station is a "Master," an additional pulse appears 2000 μsec after the 8th). Further, this group is repeated in time with period called the Group Repetition Interval (GRI), typically in the range of 50,000 to 100,000 μsec. The individual pulses in a pair of GRIs, called a Phase Code Interval (PCI), are modulated with a sequence of +1s and –1s, the so-called phase code (which eliminates the impact of long delay multipath). Finally, several geographically nearby stations will broadcast in a time-orthogonal sense at the same GRI, called a "chain". Figure 2 shows a typical observation of the Loran signal, showing the four stations in this example chain with varying amplitudes.

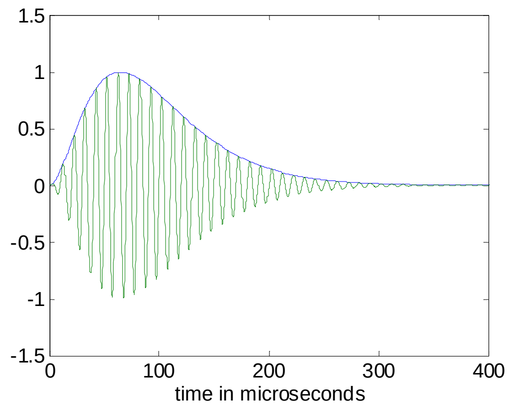

Figure 1: The Loran pulse.

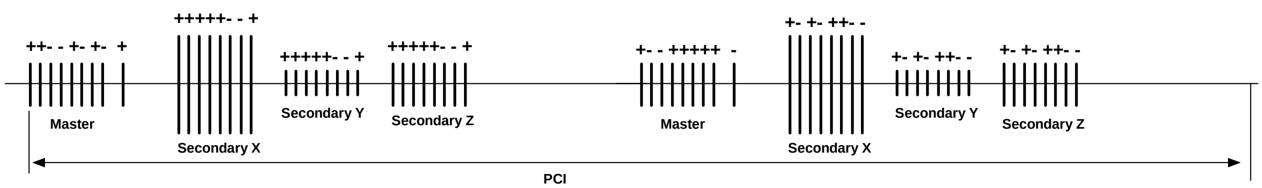

Figure 2 – A typical observation of a Loran chain.

Accurate reception of Loran signals at a user's site depends upon a variety of issues: the local signal strength relative to noise levels, interference due to Loran signals from other nearby chains with different GRIs (called cross rate interference, CRI), multipath interference of the signal itself due to ionospheric reflections (called sky wave), blanking of the signal (when a dual-rated transmitter, attempting to simultaneously send pulses from different GRIs, drops pulses on one rate), etc.

9TH PULSE LDC – ADDING DATA TO THE LORAN SIGNAL

The 9th pulse LDC system inserts an additional, non-navigation pulse into the Loran transmission along with the standard navigation pulses as shown in Figure 3 (the 9th pulse is shown in red and this is not to be confused with the extra pulse appearing in a Master group). Official documentation on this system appears in [1]. The nominal start time of the 9th pulse is 1000 μsec after the 8th navigation pulse; pulse position modulation shifts the actual start time to a later point depending upon the specific data being transmitted (hence the somewhat wider red box shown in the figure).

The 9th pulse system transmits 5 bits per Loran group via 32-ary pulse position modulation (PPM) of this extra pulse. This pulse shifting is implemented as shown in Figure 4; four "coarse" groups of 8 signals (shown in different colors) have separations of approximately 50 μsec, the "fine" timing of the 8 signals within each coarse group is approximately 1.25 μsec (22.5° of the sinusoid).

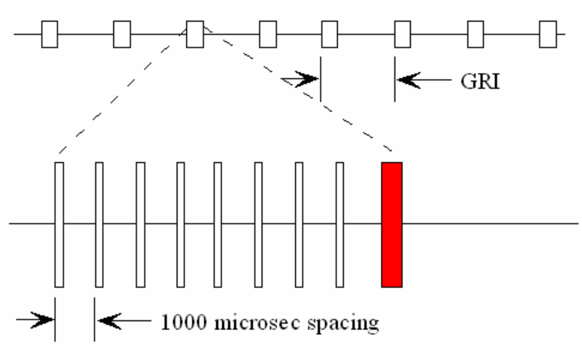

Figure 3 – A Loran group with 9th pulse LDC.

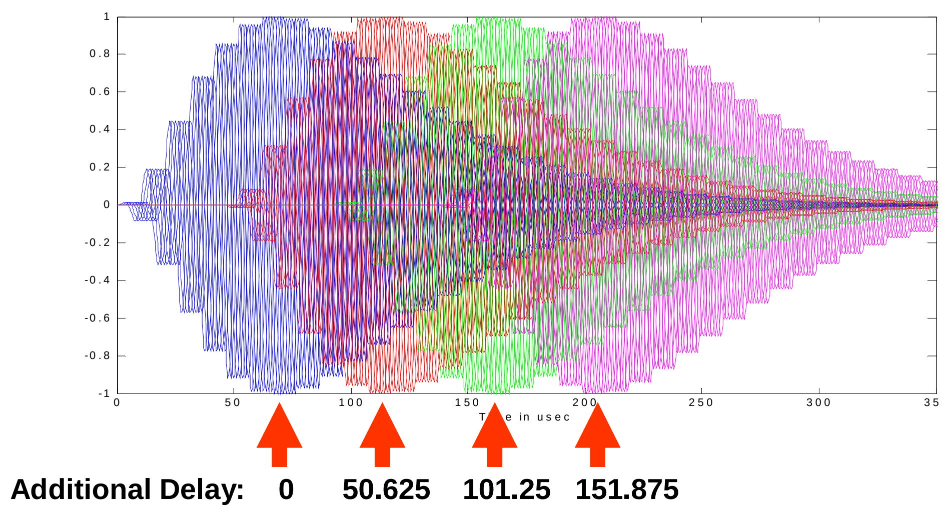

Figure 4 – Time domain versions of the 32-ary pulse position modulation.

A true signal space model for 9th pulse LDC would require a 32 dimensional signal space; prior analysis has shown that a good model for each coarse group is 8-PSK [2,3,4]. Even with this model, however, trying to represent all four sets of 8 signals in signal space at the same time would require an 8-dimensional signal space. Instead the left subfigure in Figure 5 shows a topologically correct representation of signal space; the 32 signals appearing on four concentric 8-PSK patterns. The utility of this figure is in recognizing that typical error events for any specific signal primarily involve those 6 signals closest to the one of interest (4 for those signals in the first or last set of 8): the two signals adjacent in angle in the same PSK ring and those two signals closest in angle in the two adjacent PSK rings. The right subfigure shows an example of this, connecting signal #12 to its 6 nearest neighbors.

For readers not expert in signal space theory, it is well known that errors due to additive channel noise are dominated by those signals closest in distance to the signal of interest (intuitively, channel noise is much more likely to generate a “close” error than a “far” error). An understanding of which error events are likely, then, allows the interpretation of performance results; specifically, separating out those errors due to channel noise and those due to other forms of interference in the Loran broadcast. Furthermore, it provides tools for selecting parameters in a signal design; one tries to maximize the minimum distance between all pairs of signals.

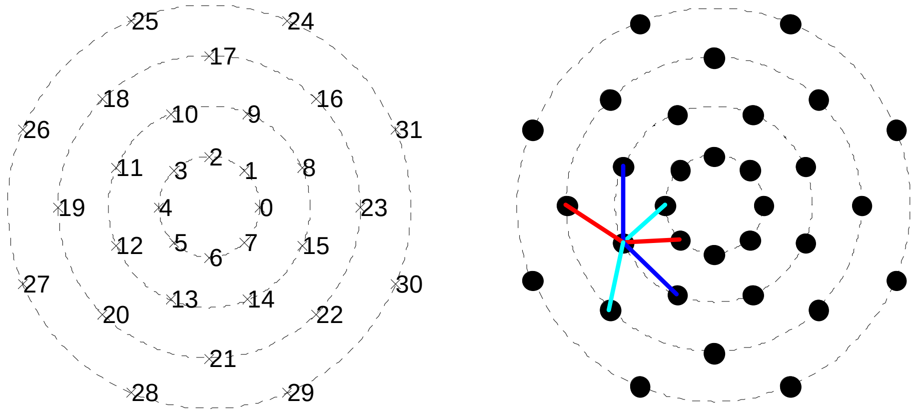

Figure 5 – A topologically accurate representation of the 32 current LDC signals; signal #12 and its six nearest neighbors.

As is typically the case for high dimension signal sets, it is impractical to exactly calculate the probability of symbol error for 9th pulse LDC; the usual approach is to upper bound the error probability using the union bound. Assuming that the channel noise can be modeled by additive white Gaussian noise, the probability of error can be bounded by

$$P_e \le \frac{1}{32}\sum_{k=1}^{32}\sum_{j\ne i} Q\left(d_{k.j}\sqrt{\frac{\gamma}{2}} \right)$$

where γ is the signal to noise ratio (SNR) and $d_{k,j}$ is the Euclidean distance between the k^{th} and j^{th} signals

$$d_{k.j} = \sqrt{\int \left(s_k(t) - s_j(t) \right)^2 dt}$$

Figure 6 shows this bound versus SNR. A coverage analysis of 9th pulse in [2] suggests that worst case SNRs in CONUS would be approximately 18 dB; most locations would see 22 dB or better. At 18 dB, the symbol error rate for 9th pulse LDC is fewer than 1 in 200.

The 9th pulse system employs forward error correction to mitigate channel effects. Specifically, a (24,9) Reed-Solomon (RS) code maps 9 data symbols (a total of 45 information bits) into 24 symbol sequences (codewords) for transmission during 24 sequential Loran groups. One significant advantage of using RS codes is their provision for erasures and errors decoding. In general, the decoding algorithm for an RS (n,k) (n is the length of the codeword in symbols, k is the number of information bearing symbols) code can correct for a combination of s erasures (such as a symbol not being sent due to blanking at the transmitter or an obvious cross rate interference collision with an adjacent rate signal) and t errors (such as generated by channel noise or untracked cross rate) as long as the error and erasure counts satisfy

$$2t + s \le n - k$$

(Conceptually, errors are twice as costly as erasures in that they must be both located and

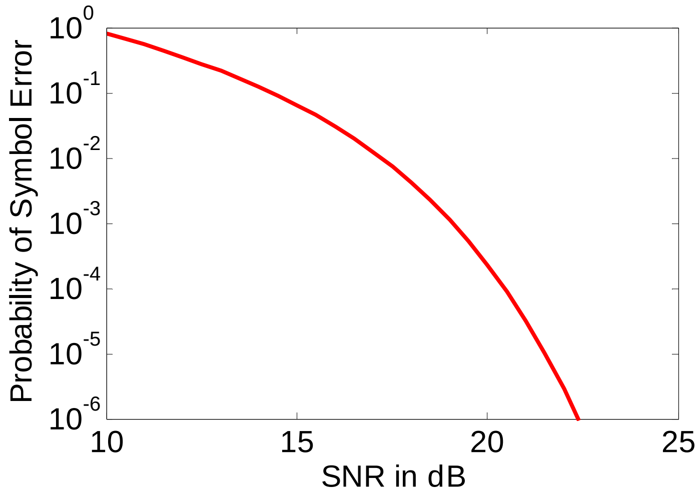

Figure 6 – Probability of error for 9th pulse LDC as a function of SNR.

corrected; erasures are, by definition, located, so need only be corrected.) For the current 9th pulse implementation, n = 24 and k = 9, so decoding succeeds if $2t + s \leq 15$. Typically the full decoding power is not used so as to provide a level of data integrity.

Experience to date suggests that 9th pulse symbol error performance is dominated by cross rate interference and blanking; erasures and errors due to these two interference modes may impact 10-20% of the received symbols. In comparison, the loss due to noise (i.e. the closeness of the adjacent signals) appears to be much less. Putting more data on each pulse or within each group could allow for more redundant symbols and, hence, better immunity to CRI, blanking, and noise. For example, currently 9th pulse LDC transmits 45 data bits (9 symbols at 5 bits per symbol) in each 24 symbol message. Increasing by one bit, to 6 bits per group, could provide 48 bits in 8 groups, yielding an extra redundancy symbol in a 24 group message which provides for more powerful errors and erasures decoding (and/or higher data integrity).

Bits could be added to 9th pulse in several ways. Two obvious methods are:

- Add a 10th pulse (nominally 2000 µsec after the 8th as suggested in the left subfigure of Figure 7)
- Add bits to the 9th pulse by allowing for more potential shifts in the PPM (as suggested by the wider red box in the right subfigure of Figure 7)

Specific discussions of both methods appear next.

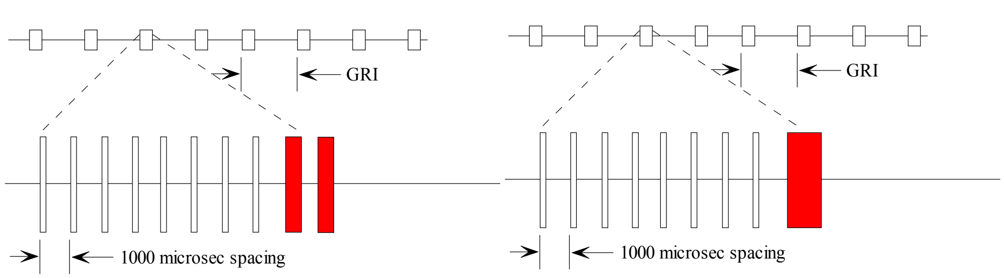

Figure 7 – A Loran group with LDC; the 9th and 10th pulses appear in red.

10^{th} Pulse

Adding a 10^{th} pulse has been discussed by Peterson in [5]. Using the same modulation method as currently is implemented for 9^{th} pulse LDC, the added 5 bits per group could be used in several ways:

- As a 32-ary symbol for a parallel and separate codeword. In this case, the analysis is no different than that above. The only change is that adjacent chains also implementing 10^{th} pulse would generate slightly more cross rate interference on the signal of interest.
- As pairs of symbols in a longer code (i.e. 24 groups yields a codeword of 48 symbols) or a shorter message (12 groups yielding the 24 symbols).
- As a "super" symbol in a code with a larger symbol set, e.g. a 1024-ary alphabet.

The first of these is not of interest here; perhaps the only interesting aspect of it is that the two messages would have highly correlated losses due to CRI. As was shown in earlier work in IFM LDC [6], the second idea (multiple symbols per group) is inferior to the third idea (supersymbols) when both pulses have similar, moderate error characteristics (i.e. hit by common CRI and not too frequently). Specifically, Shannon-theoretic arguments show that codes with larger alphabets are superior to those with more symbols of lesser extent except for very bad channels.

The analysis and testing of $9^{th}/10^{th}$ pulse LDC, then, is just verification that the transmitter can send the pulses (it can although one needs to restrict transmission to Secondary Loran transmitters only), that pairs are almost always subject to the same CRI (a short on-air trial in Fall 2008 showed nearly identical CRI erasure rates), and that one just needs to modify the error and erasure expressions for a RS code error analysis. For example, channel noise error rates change in the obvious way for pairs of independent (time orthogonal) events

$$P_e(\text{super symbol}) = 1-(1-P_e)^2 = 2P_e - P_e^2 > P_e$$

i.e. more symbol errors occur (as one would expect). Similarly, a simplistic way to view cross rate interference is that the original 9^{th} pulse window overlaps one of the 8 pulses in the interferer. If it was the 8th pulse of the interferer, then the current 10^{th} pulse window is unaffected; otherwise, the 10^{th} pulse window is also hit. In other words, ⅞'s of the time, if the 9^{th} pulse window is contaminated then so is the 10^{th} pulse window. Further, this fraction is the same for an impacted 10^{th} also resulting in an impacted 9^{th} (by symmetry). The overall chance of being hit by cross rate interference, then, goes up by a factor of 1⅛. A similar argument holds for blanking on a dual rated transmitter.

Another issue with adding a 10^{th} pulse is the concomitant addition of it being cross rate to other Loran signals. Obviously one could extend the CRI analysis in [3] to these new signal sets.

9^{th} Pulse with Added Bits

Of greater interest here is extending the PPM beyond 32-ary signaling. Given the underlying sinusoidal modulation of the pulse envelope, good PPM signal sets will still be a combination of "coarse" and "fine" shifts. As described above, the current 9^{th} pulse modulation set balances errors to adjacent signals in the same coarse set with errors to signals in adjacent coarse sets. To increase the number of bits beyond 5 requires in increase beyond 4 coarse groups and/or beyond 8 shifts per 360 degrees. Consider the following options for an increase of one bit (to 64 signals):

- Doubling the number of coarse groups – keeping the same coarse group spacing would lead to a very wide 9th pulse window, more susceptible to CRI; shrinking the coarse group spacing will allow error events between adjacent coarse groups to dominate.
- Double the number of shifts in each coarse group – shrinking the PSK separation to 12.5º would cause adjacent signal error rates to soar both due to channel noise and untracked (i.e. low power) CRI.
- Some decrease in the angular spacing within each coarse group combined with additional coarse groups with closer spacing. The coarse and fine spacing would be controlled so that errors for channel noise are still dominated by the two signals in the current PSK ring and the two signals in each adjacent coarse group.

As trial designs, two signal sets at 6 and 7 bits per pulse have been implemented. For simplicity of analysis and design, the signal sets have been based on only two parameters; the coarse time shift t_C and the fine shift t_F. To limit the range of parameter exploration, both of these have been kept on a 10 MHz clock (i.e. resolution of 0.1 μsec) and the overall range of the envelope has been contained well below 500 μsec.

Analysis of these signal sets directly parallels that above for 32-ary LDC. Figure 8 shows signal space constellations for both examples (for 64 signals, t_C = 30.4 μsec and t_F = 0.9 μsec; for 128 signals, t_C = 20.3 μsec and t_F = 0.6 μsec); because the fine spacing of both examples is smaller than that of 32-ary LDC, nearest neighbor errors are more likely. Figure 9 shows the upper bound on probability of channel error, comparing the new schemes to 32-ary LDC. Of significance is that errors are obviously more likely; the cost of adding 1 and 2 bits per group are approximately 3 dB and 6.5 dB, respectively (a short on-air trial in Fall 2008 verified this rather obvious statement). If the minimum SNR in the coverage area is high enough, these error rates may still be low enough when compared to erasures and errors due to CRI and blanking so that the errors do not dominate overall system performance. For example, at 22 dB SNR, the 6 bit per symbol signal set would experience only about a one in one-thousand symbol error rate.

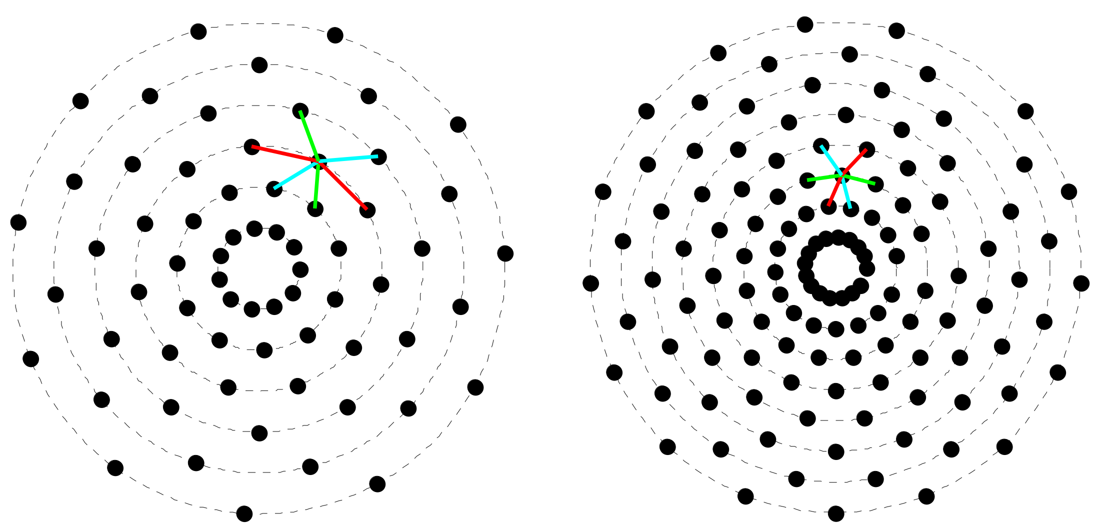

Figure 8 – A topologically accurate representation of the proposed 64-ary and 128-ary LDC signals; one typical signal and its six nearest neighbors are marked in each.

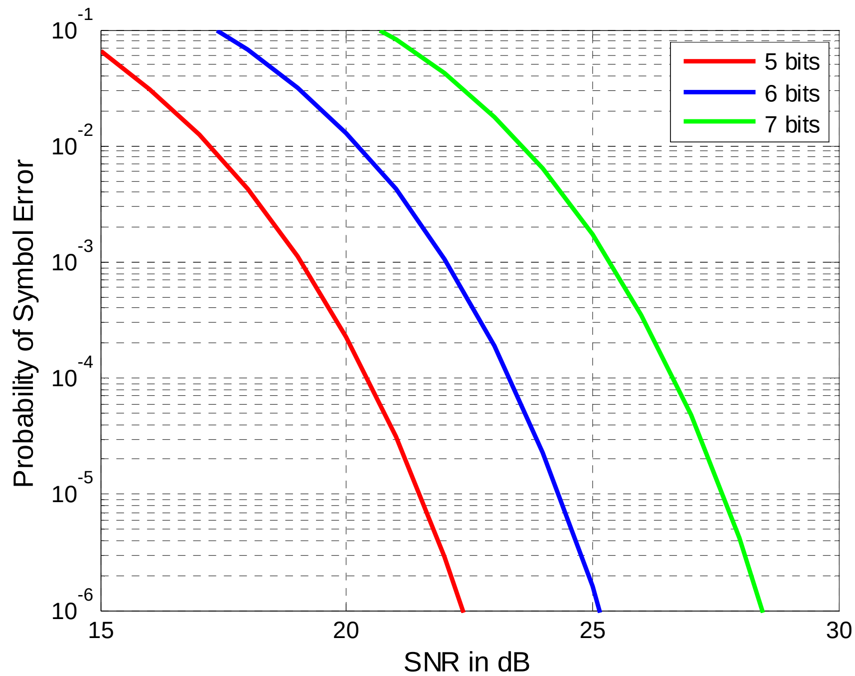

Figure 9 – Probability of error as a function of SNR for the three modulation sets of interest.

EFFECTS OF UNBALANCED PHASE CODES

In 1975 Feldman [7] first presented a Fourier analysis of Loran, showing the interrelationships of the pulse shape, the phase code, and the GRI on the resulting spectrum. Recently, at the IEEE/ION PLANS 2008 [8], these authors revisited this analysis, arguing that "balanced" phase codes should be implemented for *e*Loran. This section begins with the results of a Fourier Series analysis of the Loran signal, with emphasis on the impact of cross rate interference. The details of the analysis are delegated to the Appendices; Appendix A repeats (and corrects) the material originally presented in [8] and Appendix B extends those arguments to show the precise impact of the lack of balance on other *e*Loran signals.

Summary of the Results

Recall that the Loran signal is periodic on a PCI; hence, it can be fully described by a Fourier Series representation. The common envelope of the Loran pulse determines the envelope of the resulting spectrum, the PCI determines the relative spacing (equal to 1/PCI Hz) of the individual spectral lines under that envelope, and the phase code determines the fine structure of the spectrum. The analytical result for the currently implemented Secondary phase code is

$$s(t) = \sum_{n=-\infty}^{\infty} \alpha_n \sin\left(2\pi\left(0.1 + n / PCI\right)t + \beta_n\right)$$

with $d_n = \alpha_n \exp(j\beta_n)$ and

$$d_n = \begin{cases} \dfrac{65e^2 PCI^2}{4(PCI + j65\pi n)^3}\left[1 + e^{-j2\pi n 2000/PCI} + e^{-j2\pi n 4000/PCI} - e^{-j2\pi n 6000/PCI}\right] & n \text{ even} \\ \dfrac{65e^2 PCI^2}{4(PCI + j65\pi n)^3}\left[e^{-j2\pi n 1000/PCI} + e^{-j2\pi n 3000/PCI} - e^{-j2\pi n 5000/PCI} + e^{-j2\pi n 7000/PCI}\right] & n \text{ odd} \end{cases}$$

As an example of this result, the left subfigure of Figure 10 shows the line spectrum for the 9960 chain (GRI = 99,600 μsec); individual lines are spaced at the reciprocal of the PCI, 5.02 Hz in this case. Rather than show the full spectrum, this plot displays the magnitudes of the upper sideband's lines, from 100 kHz to 110 kHz, in the band allocated for Loran (the abscissa is parameterized as the offset from 100 kHz). At this scale, individual lines are impossible to see. The right hand subfigure shows a portion of this same spectrum, 100 kHz to 100.2 kHz to demonstrate the fine detail in the lines' heights due to the phase code.

It is obvious from the series expression that all Loran signals (with the current Secondary phase code) have a component at 100 kHz. Further, signals with different PCIs will also share common spectral lines spaced at the reciprocal of their greatest common divisor. Any linear (averaging) receiver will be unable to directly cancel these common lines; hence, allowing interfering energy from another Loran chain into processing of the one of interest.

In the US, all GRIs are a multiple of 100 μsec, so the PCIs are all a multiple of 200 μsec and minimally have 200 μsec as their greatest common divisor; the implication is that all US Loran signals have common spectral lines at multiples of 5 kHz. For some pairs of PCIs, common frequencies can occur more frequently (e.g. for GRIs of 7980 and 9960 the common frequencies are all multiples of 833.333 Hz). The amplitudes of the lines at multiples of 5 kHz, with $n = 5m$*PCI/1000 for integer m, is

$$d_n = \frac{65e^2}{4(PCI + j65\pi n)^3}\left(\sum_{k=0}^{7} b_k \pm \sum_{k=8}^{15} b_k\right)$$

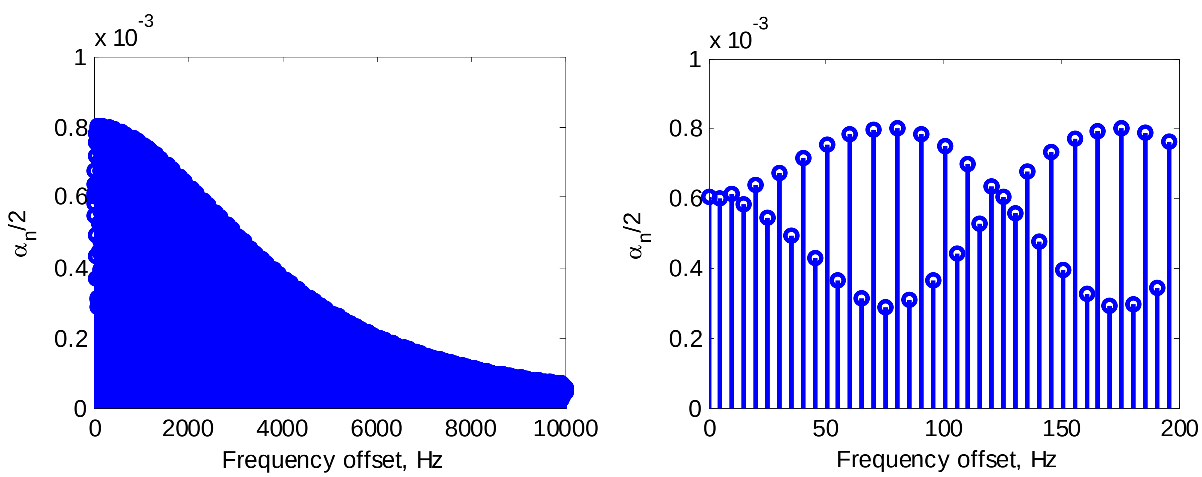

Figure 10 – Magnitude spectrum for the 9960 Loran signal; a zoomed in look at part of that spectrum.

(again, use the plus sign for even n and the minus sign for odd n). If the phase code is balanced on the two separate groups, b_0 through b_7 and b_8 through b_{15}, then the sum in parentheses equals zero and all lines at multiples of 5 kHz are zeroed out irrespective of whether or not n is even or odd. As an example, the following phase code satisfies this property.

$$\begin{aligned}[b_0, b_1, b_2, \ldots b_7] &= [+1, -1, +1, +1, -1, +1, -1, -1] \\ [b_8, b_9, b_{10}, \ldots b_{15}] &= [+1, +1, +1, -1, -1, -1, -1, +1]\end{aligned}$$

Note that while not mitigating sky wave impact for all delays, this phase code does protect for delays ranging from 500 μsec to 3700 μsec (effectively covering all cases of interest) [8].

The Impact of Balance on TOA Estimation

If two nearby chains share common spectral lines, then simple linear averaging methods will not completely cancel both noise and cross rate interference. For example, imagine a receiver tracking a station at rate R_1 and amplitude A_1 using data contaminated by a signal at rate R_2 and amplitude A_2 (and arriving at some other point in time). If the receiver does linear averaging, and the time constant of the receiver is long enough, then its effect is to eliminate all energy except for that present at the locations of the line spectrum of the signal of interest. Letting $s_1(t)$ and $s_2(t)$ be the two signals, then $s_1(t)$ is undisturbed and $s_2(t)$ is reduced to only its components at these common spectral lines

$$s_2(t) = A_2 \sum_{n=-\infty}^{\infty} d_n e^{j2\pi nt/PCI} \Rightarrow r_2(t) = A_2 \sum_{m \in M} d_n e^{j2\pi n(t+\tau)/PCI}$$

In this expression, $r_2(t)$ is the residual signal and M describes the set of common spectral lines. Note that a time shift τ appears in this expression to account the fact that the second Loran signal comes in with a time offset relative to the signal of interest.

As an example, consider the situation of two Loran PCIs whose greatest common divisor is 200 μsec; equivalently, the spectral lines remaining in $r_2(t)$ appear only at integer multiples of 5 kHz. Referring to Appendix B for details, keeping just the lines within the nominal Loran range (90-110 kHz), this residual signal is

$$r_2(t) \approx A_2 \sum_{m=-2}^{2} \alpha_{(m)} \sin\left(2\pi(0.1 + 0.005m)(t+\tau) + \beta_{(m)}\right)$$

where

$$\begin{aligned}\alpha_{(m)} &= \left|d_{(m)}\right| = \frac{65e^2}{PCI\left(1 + 0.325^2\pi^2 m^2\right)^{3/2}} \\ \beta_{(m)} &= angle(d_{(m)}) = -3\tan^{-1}(0.325\pi m)\end{aligned}$$

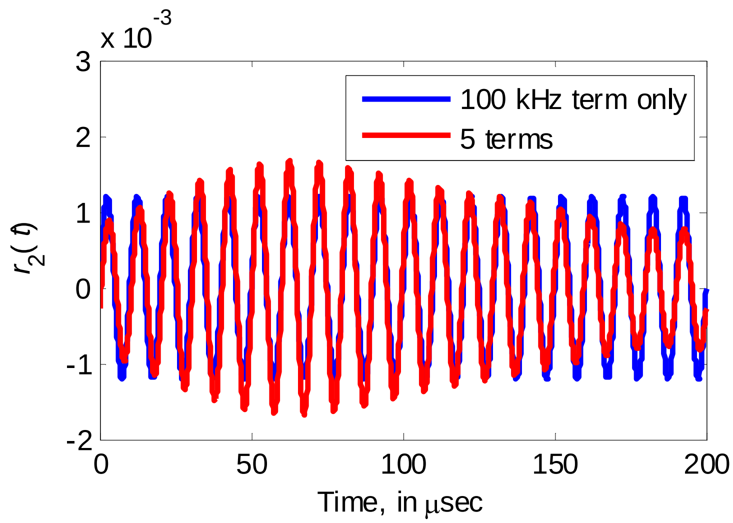

Figure 11 – The residual signal due to the 100 kHz line and that due to the common lines at multiples of 5 kHz.

Figure 11 shows this signal versus time for $A_2 = 1$ and $\tau = 0$. As expected, since it is dependent upon lines at multiples of 5 kHz, this signal is periodic on 200 μsec. This figure also shows the interference from just the 100 kHz tone alone, relevant for pairs of chains whose greatest common divisor of the PCIs results in other common lines being all outside of the 90-110 kHz band.

Of significance is how this signal effects reception of $s_1(t)$. Figure 12 shows both $s_1(t)$ alone (the blue line) and $s_1(t) + r_2(t)$ (the red line) where the time shift $\tau = -32.5$ μsec is selected so that the maximum of $r_2(t)$ occurs at the 3rd zero crossing of $s_1(t)$ (the 30 μsec point). It is clearly seen that the presence of the residual energy moves the 3rd zero crossing by some 42 nsec! Also shown in green is the interference effect if only the 100 kHz line was present (i.e. the blue interference function in Figure 11 shifted by –2.5 μsec); still an error of 30 nsec. (Of course, this is worst case in that a different time offset between the signal of interest and the interferer, constructive interference, could result in zero error.) The amplitude ratio A_2/A_1 for both the red and green curves in Figure 12 is 10; i.e. the interfering Loran signal is 20 dB stronger than the signal of interest (not an unrealistic value). The rate of the interferer in this example is 9960. A close look at the analysis shows that the level of interference depends upon the rate of the interferer; for example, with a 5930 interferer, the offsets increase to 71 nsec for 5 sinusoid interference and 52 nsec for the 100 kHz line alone.

A test using different phase codes was conducted at the Loran Support Unit during Fall 2008 in order to verify the above analysis. Specifically, a test transmitter capable of altering its phase code was operated on LSU's test rate of 5030; simultaneously, raw Loran data was captured at the nearby Atlantic City airport (ACY). At ACY, the LSU signal was the dominant signal; easily 10 or more times the amplitude of the other observable Loran signals. After PCI averaging of the data, one would expect to see residual cross rate energy due to the strong LSU signal; further, the residual interference should exhibit a 200 μsec periodicity. With a balanced phase code (such as the one listed above), one would expect the interference to disappear after PCI averaging.

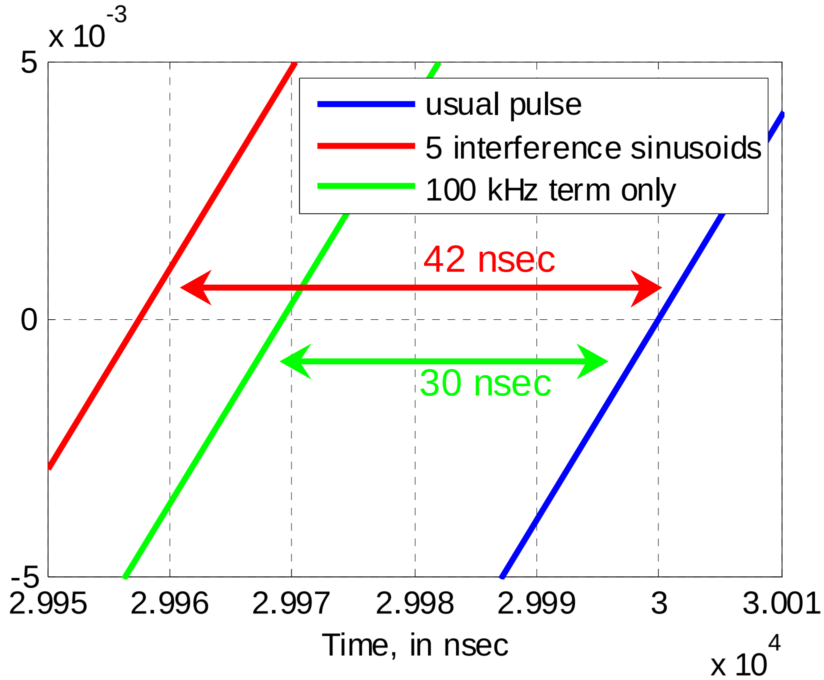

Figure 12 – The received signal near the 3rd zero crossing (30 μsec point) with residual cross rate interference.

Figures 13 and 14 demonstrate these effects. Specifically, the two plots show the results after 5 minutes of PCI averaging (actually, the lowpass equivalent signals) of the 9960 chain; Master (Seneca), Xray (Nantucket), and Yankee (Carolina Beach) are clearly visible, Zulu (Dana) also appears after this much averaging. Figure 13 shows two 5 minute averages; the blue line (mostly under the red) is the average with 5030 transmitting with the current Secondary phase code while the red line is the average with 5030 transmitting with a balanced phase code (the horizontal axis is time in samples, 10 μsec spacing, and the vertical scale is voltage). The data corresponding to the pulse locations is nearly equivalent; of significance are the portions when no Loran pulses are

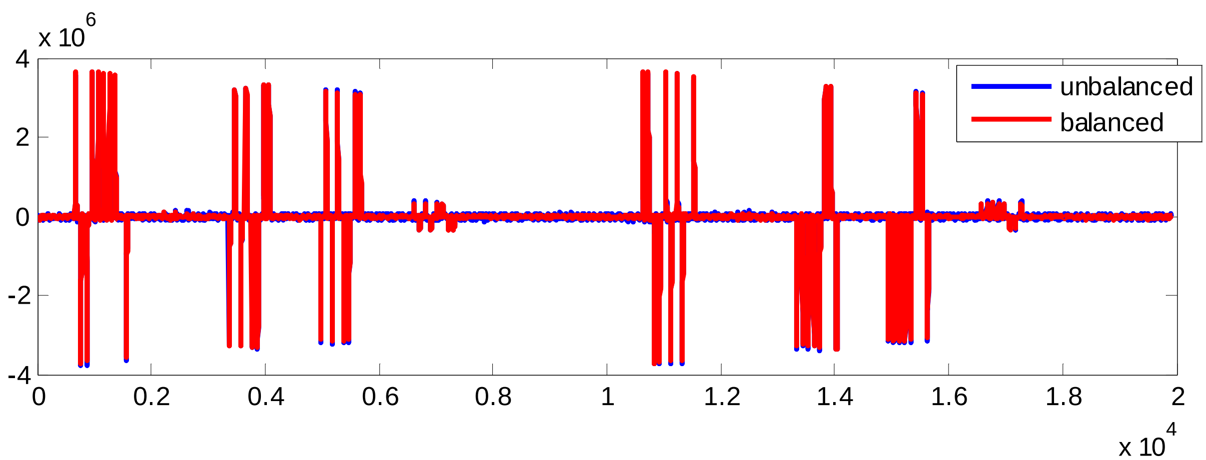

Figure 13 – PCI averaging of the 9960 chain.

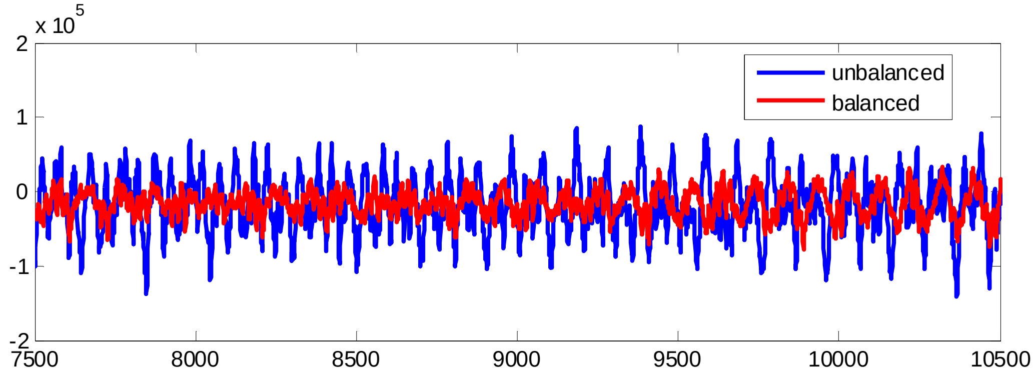

Figure 14 – PCI averaging of the 9960 chain – balanced 5030 phase code.

present. Figure 14 zooms into one such segment; a strong 5 kHz periodicity is visible in both curves. The blue curve is dominated by the interference from LSU's 5030 residual; however, removing this (i.e. going to a balanced phase code resulting in the red line) does not remove all of the interference in this example since other chains observable at ACY (5930, 7980, and 8970) contribute periodic interference to the 9960 average.

CONCLUSIONS/FUTURE WORK

This paper looked at two issues: adding data rate to the Loran data channel and how the currently unbalanced phase codes interfere with accurate TOA estimation:

- Bits could be added to the 9th pulse LDC in several ways: adding an additional 10th pulse to LDC and increasing the size of the signal set of the 9th pulse. The 10th pulse approach adds rate at the cost of increased CRI to other signals (its impact is yet to be explored). Increasing the modulation set size of the 9th pulse is certainly possible; the presented 64-ary scheme has the potential to yield redundancy with acceptable error rates.
- As was noted previously in [8], balanced phase codes have been shown to eliminate a significant amount of cross rate interference; the cost in diminished sky wave protection seems a small price to pay.

Limited on-air testing with a transmitter at LSU reinforced these results.

DISCLAIMER

The views expressed herein are those of the authors and are not to be construed as official or reflecting the views of the U.S. Coast Guard or any agency of the U.S. Government.

REFERENCES

1. B. Peterson, K. Dykstra, D. Lown, and K. Shmihluk, "Loran data channel communications using 9th pulse modulation (ver 1.3)," USCG Loran Support Unit, Wildwood, NJ, 20 Oct. 2006.
2. L. Hartshorn, P. Swaszek, G. Johnson, et al., "Performance of Loran-C 9th pulse modulation techniques," *Proc. ION NTM*, Monterey, CA, 18-20 Jan. 2006.
3. M. Kuhn, P. Swaszek, G. Johnson, et al., "Performance analysis and potential improvements of the Loran Data Channel," *Proc. ION NTM*, Cambridge, MA, 23-25 Apr. 2007.
4. P. Swaszek, G. Johnson, K. Dykstra, et al. "Improved signal processing methodologies for the Loran Data Channel", *Proc. ION NTM*, San Diego, CA, 28-30 Jan. 2008.
5. B. Peterson, "White paper on additional modulated pulses for increased messaging capacity," unpublished, 21 June 2007.
6. B. Peterson, K. Dykstra, P. Swaszek, and J. Boyer, "High speed Loran-C data communications June 2001 update," *Proc. ION AM*, Albuquerque, NM, 11-13 June 2001.
7. D. A. Feldman, P. E. Pakos, and C. E. Potts, "On the analysis and minimization of mutual interference of Loran-C chains," *Proc. Annual Tech. Symp. Wild Goose Assoc.*, Cockeysville, MD, 16-17 October 1975.
8. P. Swaszek, G. Johnson, and R. Hartnett, "Loran phase codes, revisited," *Proc. IEEE/ION PLANS*, Monterrey, CA, 5-8 May 2008.

APPENDIX A – FOURIER ANALYSIS OF LORAN

In 1975, Feldman [12] presented a Fourier analysis of Loran, showing the interrelationships of the pulse shape, the phase code, and the GRI on the resulting spectrum. This appendix clarifies and expands on that analysis. (Note that these authors present a similar analysis in [8] and that that presentation contains a minor typographical error which is corrected here.)

Recall that the Loran signal is periodic on a PCI; hence, it can be fully described by a Fourier Series representation. To develop a simple expression for this expansion, start with a single Loran pulse, $p(t)$, starting at time zero in the PCI. Ignoring the modulation by 100 kHz for the moment, the Fourier Series can be written as

$$p(t) = \sum_{n=-\infty}^{\infty} c_n e^{j2\pi nt/PCI} \qquad \text{with} \qquad c_n = \frac{1}{PCI}\int_0^{PCI} p(t) e^{-j2\pi nt/PCI} dt$$

For the standard expression of the Loran envelope (assuming that time t is measured in μsec)

$$p(t) = \frac{t^2 e^{-2t/65}}{65^2 e^{-2}} u(t)$$

(note that the scaling yields a unit maximum pulse) the coefficient reduces to

$$c_n = \frac{65e^2 PCI^2}{4(PCI + j65\pi n)^3}$$

From this expression, the spectrum of a single pulse is seen to consist of very many lines (spacing of 1/PCI in Hz, 5.02 Hz for the 9960 GRI) with monotonically decreasing magnitudes; the envelope of this function falls little until n becomes large (i.e. for typical Loran PCIs, there may be 200 or more lines before the amplitude hits one-half of its $n = 0$ value).

Actually, the Loran PCI consists of 16 such pulses

$$p_{16}(t) = \sum_{m=0}^{15} b_m p(t - \tau_m)$$

where the b_m are the phase code terms ($b_m = \pm 1$) and the τ_m account for both the 1000 μsec spacing between pulses within each of the two groups in the PCI and the GRI spacing between the two groups. In the frequency domain, adding a time shift of τ_m results in a phase shift in the Fourier coefficients. Also, by linearity, the multiplication by b_m directly modifies the coefficient; hence, the combined result is a scaling of each coefficient from the expansion of the original pulse

$$c_n \rightarrow c_n b_m e^{-j2\pi n \tau_m / PCI}$$

and that the Fourier Series of the sum equals the sum of the 16 individual Fourier Series

$$p_{16}(t) = \sum_{n=-\infty}^{\infty} d_n e^{j2\pi nt/PCI} \qquad \text{with} \qquad d_n = c_n \sum_{m=0}^{15} b_m e^{-j2\pi n \tau_m / PCI}$$

Clearly, the final spectrum for a particular GRI depends upon the summation in the expression for d_n. Now, since the PCI is equal to twice the GRI, the 8 final pulses have

$$\begin{aligned} e^{-j2\pi n \tau_m / PCI} &= e^{-j2\pi n (PCI/2 + 1000m)/PCI} \\ &= e^{-j\pi n} e^{-j2\pi n (1000m)/PCI} \\ &= \begin{cases} -e^{-j2\pi n(1000m)/PCI} & ;n \text{ odd} \\ e^{-j2\pi n(1000m)/PCI} & ;n \text{ even} \end{cases} \end{aligned}$$

and

$$\begin{aligned} \sum_{m=0}^{15} b_m e^{-j2\pi n \tau_m / PCI} &= (b_0 \pm b_8) + (b_1 \pm b_9) e^{-j2\pi n 1000/PCI} \\ &+ (b_2 \pm b_{10}) e^{-j2\pi n 2000/PCI} + (b_3 \pm b_{11}) e^{-j2\pi n 3000/PCI} \\ &+ (b_4 \pm b_{12}) e^{-j2\pi n 4000/PCI} + (b_5 \pm b_{13}) e^{-j2\pi n 5000/PCI} \\ &+ (b_6 \pm b_{14}) e^{-j2\pi n 6000/PCI} + (b_7 \pm b_{15}) e^{-j2\pi n 7000/PCI} \end{aligned}$$

where the plus sign is used for even n and the minus sign for odd n.

The final step is to modulate this baseband signal to 100 kHz

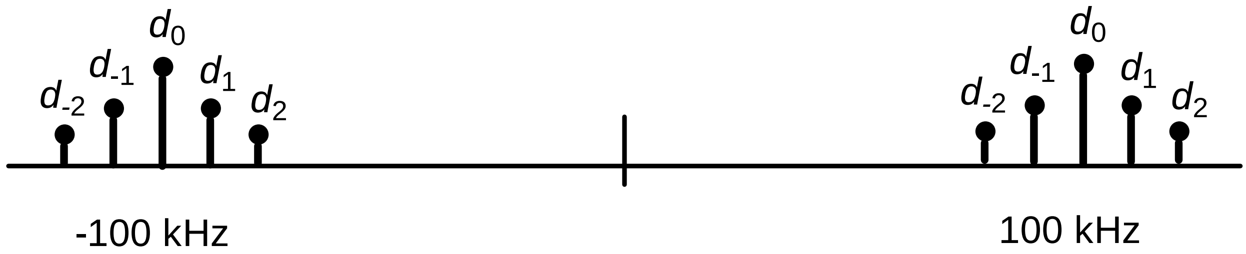

Figure A1 – Fourier Series representation of Loran; only 5 spectral lines are shown for simplicity.

$$s(t) = p_{16}(t)\sin 0.2\pi t$$

Employing the standard Euler expansion for the sine

$$\sin\phi = \frac{e^{j\phi} - e^{-j\phi}}{2j}$$

in the Fourier Series expansion for the 16 pulses yields

$$\begin{aligned} s(t) &= \sum_{n=-\infty}^{\infty} \frac{d_n}{2j} e^{j2\pi nt/PCI}\left(e^{j0.2\pi t} - e^{-j0.2\pi t}\right) \\ &= \sum_{n=-\infty}^{\infty} \frac{d_n}{2j}\left(e^{j2\pi(0.1+n/PCI)t} - e^{-j2\pi(0.1-n/PCI)t}\right) \end{aligned}$$

The result is spectral lines displaced in both directions from both ±100 kHz at spacings of 1/PCI Hz. The first few lines on each side are shown in Figure A1, a standard "lollipop" representation for the series (note that the scaling by 1/2*j* is dropped for clarity).

The expression for $s(t)$ can be manipulated, combining common frequency terms

$$\begin{aligned} s(t) &= \sum_{n=-\infty}^{\infty} \frac{d_n}{2j} e^{j2\pi(0.1+n/PCI)t} - \sum_{n=-\infty}^{\infty} \frac{d_n}{2j} e^{-j2\pi(0.1-n/PCI)t} \\ &= \sum_{n=-\infty}^{\infty} \frac{d_n}{2j} e^{j2\pi(0.1+n/PCI)t} - \sum_{n=-\infty}^{\infty} \frac{d_{-n}}{2j} e^{-j2\pi(0.1+n/PCI)t} \\ &= \sum_{n=-\infty}^{\infty} \frac{d_n e^{j2\pi(0.1+n/PCI)t} - d_{-n} e^{-j2\pi(0.1+n/PCI)t}}{2j} \end{aligned}$$

From the definition of d_n, $d_{-n} = d_n^*$. Further, write $d_n = \alpha_n \exp(j\beta_n)$ to yield

$$
\begin{aligned}
s(t) &= \sum_{n=-\infty}^{\infty} \frac{\alpha_n e^{j\beta_n} e^{j2\pi(0.1+n/PCI)t} - \alpha_n e^{-j\beta_n} e^{-j2\pi(0.1+n/PCI)t}}{2j} \\
&= \sum_{n=-\infty}^{\infty} \alpha_n \frac{e^{j(2\pi(0.1+n/PCI)t+\beta_n)} - e^{-j(2\pi(0.1+n/PCI)t+\beta_n)}}{2j} \\
&= \sum_{n=-\infty}^{\infty} \alpha_n \sin\left(2\pi(0.1+n/PCI)t+\beta_n\right)
\end{aligned}
$$

The result is a sinusoidal representation for the Loran signal.

APPENDIX B – SPECTRAL LINES AT MULTIPLES OF 5 KHZ

While the analysis in Appendix A referred to a single Loran signal (or chain), it is of interest to look further at those spectral lines common to multiple chains. In the US, all GRIs are a multiple of 100 μsec, so the PCIs are all a multiple of 200 μsec and minimally have 200 μsec as their greatest common divisor; the implication is that all US Loran signals have common spectral lines at multiples of 5 kHz. Of these, the lines at 90, 95, 100, 105, and 110 kHz all have significant power levels. In Europe (and elsewhere) GRIs whose greatest common divisor is only 10 μsec would yield overlapping lines at 50 kHz offsets; hence, for those locations only the line at 100 kHz is both significant and common.

Continuing for the US situation, this appendix further examines the components at the 5 kHz spacing. The goal is to describe the effects of cross rate interference that are not removed by linear averaging (in other words, why receiver manufacturers need to apply more advanced non-linear processing) so as to make a convincing argument for altering the phase codes currently in use.

For an offset of 5*m* kHz (i.e. *m* an integer) from 100 kHz, the corresponding index in the series expansion corresponds to $n = 5m$*PCI/1000; the residual signal when only keeping these spectral lines is

$$
r(t) = \sum_{m=-\infty}^{\infty} \alpha_{5mPCI/1000} \sin\left(2\pi(0.1+0.005m)t + \beta_{5mPCI/1000}\right)
$$

Of significance are the lines for $m = 0, \pm 1, \pm 2$, the lines within the 90-110 kHz Loran band. The coefficients for these lines are

$$
d_{5mPCI/1000} = c_{5mPCI/1000} \begin{bmatrix} (b_0 \pm b_8) + (b_1 \pm b_9)e^{-j2\pi 5m} \\ + (b_2 \pm b_{10})e^{-j2\pi 10m} + (b_3 \pm b_{11})e^{-j2\pi m 15m} \\ + (b_4 \pm b_{12})e^{-j2\pi 20m} + (b_5 \pm b_{13})e^{-j2\pi 25m} \\ + (b_6 \pm b_{14})e^{-j2\pi 30mI} + (b_7 \pm b_{15})e^{-j2\pi 35m} \end{bmatrix}
$$

Since all of the exponents within the bracketed term are integer multiples of 2π, all of the exponentials equal unity and the coefficients reduce to

$$d_{5mPCI/1000} = \frac{65e^2}{4PCI\left(1+j0.325\pi m\right)^3}\left(\sum_{k=0}^{7} b_k \pm \sum_{k=8}^{15} b_k\right)$$

(again, use plus for even *n* and minus for odd *n*). For the existing Secondary phase code, the two sums in the parentheses are 4 and 0, respectively, so

$$d_{5mPCI/1000} = \frac{65e^2}{PCI\left(1+j0.325\pi m\right)^3}$$

If one used a "balanced" phase code, such as

$$\left[b_0, b_1, b_2, \ldots b_7\right] = \left[+1,-1,+1,+1,-1,+1,-1,-1\right]$$
$$\left[b_8, b_9, b_{10}, \ldots b_{15}\right] = \left[+1,+1,+1,-1,-1,-1,-1,+1\right]$$

then the coefficient for all of these spectral lines is identically zero.

Returning to the existing Secondary phase code,

$$\alpha_{(m)} = \left|d_{(m)}\right| = \frac{65e^2}{PCI\left(1+0.325^2\pi^2 m^2\right)^{3/2}}$$
$$\beta_{(m)} = angle(d_{(m)}) = -3\tan^{-1}\left(0.325\pi m\right)$$

and the "residual" signal (after linear averaging) is

$$r(t) \approx \sum_{m=-2}^{2} \alpha_{(m)} \sin\left(2\pi\left(0.1+0.005m\right)t + \beta_{(m)}\right)$$

If one is only interested in the 100 kHz line, the "residual" sinusoid is

$$r_{100}(t) \approx \frac{65e^2}{PCI}\sin\left(0.2\pi\, t\right)$$